Influence of aging on SEI and charge transfer resistances and their dependence on current and temperature for a Li-ion NCA+NMC/graphite cell

Fernanda Vendrame, Nicolas Damay, Houssam Rabab, Christophe Forgez, Marie Sayegh

Influence of aging on SEI and charge transfer resistances and their dependence on current and temperature for a Li-ion NCA+NMC/graphite cell

Fernanda Vendrame[1,2,*], Nicolas Damay[1], Houssam Rabab[1], Christophe Forgez[1], and Marie Sayegh[2]

[1] *Université de Technologie de Compiègne, Roberval (Mechanics, Energy and Electricity) , Centre de Recherches Royallieu, CS 60319, 60203 Compiègne Cedex, France*
[2] *Safran Electrical & Power , 70-80 Rue Auguste Perret, 94000 Créteil, France*
[*] Corresponding author: fernanda.vendrame@safrangroup.com

Abstract

Modeling the electrical behavior of cells is often complex because several parameters have to be determined simultaneously, which may lead to inconsistencies and inaccuracies. In the present paper, we modeled the surface resistance by using a method based on rules of dependence, already presented in the literature, which makes it possible to separate the contributions of the SEI (Solid Electrolyte Interphase) layer and the charge transfer as a function of the temperature and the current. A physically consistent model is able to provide a better estimate of the surface resistance values at untested operating points. The main contributions of this work are to transpose this method to an NCA+NMC / graphite+SiO cell and to show that the proposed model is easier to recalibrate as the cell ages than interpolation tables. Besides, the proposed experimental protocol reduces the time needed for testing. By testing cells at different states of health, it was observed that the charge transfer resistance increased with both cycling and calendar aging and that the SEI resistance also increased in both cases because of the high temperatures to which the cells were subjected.

1 Introduction

An accurate and physically coherent model of lithium-ion cells is a key element to understand the impact of operating conditions on their behavior, which may be very useful for determining crucial information such as the cell state of charge, state of health, among other indicators.

The electrical behavior of a battery can be modeled by an equivalent electrical circuit. The values of the parameters of this model depend on many factors, such as temperature, current, state of charge and state of health. Many tests are usually necessary in order to obtain the values of these parameters at different operating conditions and the results can be presented in the form of an interpolation table which will be all the more precise as the tests are numerous. However, this method presents three problems: (1) it is difficult to recalibrate these interpolation tables as the battery ages, (2) a linear interpolation between two points may give an inaccurate value of the parameter and (3) the parameters values are usually found by using optimization algorithms which usually provide solutions that are mathematically coherent, but are not necessarily physically coherent.

To address these issues, Damay *et al.* [1] proposed a method for studying one of the parameters of the electrical model, namely the surface resistance, which establishes some rules of dependence, making it possible to find a physically coherent equation of this parameter as a function of current and temperature. This method eliminates the problem of interpolation, reduces the number of tests required and forces the parameter to have a physical coherence. So, it is easier to adapt the model as the battery ages.

The present paper has two main objectives. The first objective is to show that this method, originally proposed using a pristine LFP / graphite cell, can be transposed to another chemistry, namely NCA+NMC / graphite+SiO. The second objective is to determine whether the model remains consistent at different states of health. We should then be able to quantify the effects of cycling and calendar aging on the resistances related to the SEI (Solid Electrolyte Interphase) layer and to the charge transfer phenomena.

In the next section, the battery model is presented. Its structure is detailed, as well as the methods and experimental tests needed in order to obtain its parameters. Section 3 is focused on the surface resistance, which is one of the parameters of the battery model. The physical laws that describe its behavior as a function of temperature and current are presented in order to identify the individual contributions of SEI layer and charge transfer phenomena. Finally, the results of this analysis are presented in section 4, followed by a discussion about the impact of aging over these two contributions. Some perspectives are also presented to guide the next steps of this research.

2 Battery model

2.1 Equivalent electrical circuit

There are multiple ways of representing the behavior of a cell, such as an electrochemical model [2], a data-driven model [3] or an equivalent electrical circuit model [4]. For this study, the last option was chosen. The model, represented in Fig. 1, is composed of the following elements:

- U_{oc}: a voltage source representing the OCV (open circuit voltage). This is the voltage of the cell in open circuit and at equilibrium.
- R_s: a series resistance representing all purely resistive contributions, such as electrolyte, current collectors and contact resistances.
- R_{surf}: a surface resistance related to the voltage drop between the surface of the active material and the electrolyte, due to charge transfer and SEI [1].
- $\tau_{surf} = R_{surf} \cdot C_{surf}$: a time constant related to the surface phenomena, which are associated with charge transfer, double layers and SEI. It represents a quick dynamic, usually inferior to 1 second.
- Z_{diff}: impedance related to the phenomena of lithium ions diffusion in the electrolyte and lithium atoms in both electrodes, having a slow dynamic, usually in the order of several minutes.

Once R_{surf} is identified, its behavior for different current rates and temperatures can be studied. Its dependence on SOC has not yet been analyzed, so it will not be addressed in the present paper. However, EIS (Electrochemical Impedance Spectroscopy) tests are a simple way to observe, for a given cell, whether the surface resistance has a strong depends strongly on SOC. Taking the cell used in this work as an example, its surface resistance varies very slightly between SOC 10% and 70%, so the proposed method could be applied at a SOC value within this range and some additional values closer to 0% and 100% depending on the requirements of the application.

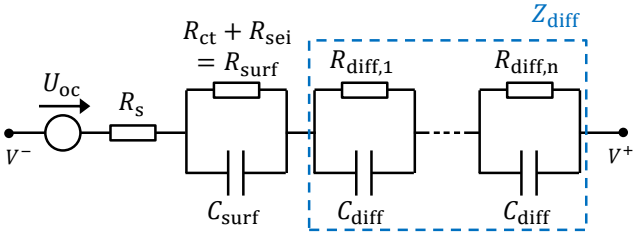

Figure 1: Equivalent electrical circuit

2.2 Experimental protocol

Three Samsung 18650-25R cells were used for this study. These are NCA+NMC/graphite+SiO cells [5] with a nominal capacity C_{nom} of 2.5 Ah, nominal voltage U_{nom} of 3.6 V, maximum current rate of 8C for continuous discharge and 1.6C for continuous charge. Each one of these cells has a different state of health ($SOH = C/C_{nom}$) :

- Cell A : SOH 100%.
- Cell B : SOH 95%. Mixed cyling and calendar aging. The cycling current rates varied between C/2 and 5C for room temperatures going from 0°C to 50°C, with maximum cell temperature reaching 70 °C.
- Cell C : SOH 87%. Calendar aging at 60°C and SOC 100% during 55 days.

A Bio-Logic system was used for tests (VSP-300) with a 20 A booster. The precision of this device is 0.1% of its full scale. Besides, the cells were placed into a climatic chamber to control their temperatures.

The experimental protocol, applied at three different temperatures (25°C, 0°C, -10°C) consists of three main parts:

1. Initialization
2. EIS
3. Current pulses in charge and discharge

For the first part, the temperature was set to 25°C, the cell was fully discharged and then charged up to 2 Ah (80% of the nominal capacity).

For the second part of the protocol, the climatic chamber was adjusted to perform the tests at the temperatures mentioned above. The EIS tests consists of applying a sine current wave to the cell and measuring its voltage variation in order to compute its impedance. This test was performed from 10 kHz to 10 mHz at C/5 and C/50. The reason for using different currents is that the lower the current, the more reasonable it is to admit that the impedance is identified at zero current, especially at very low temperatures. However, such low currents tend to cause imprecise measurements at higher frequencies, where series resistance is identified. So, when processing the EIS results, the spectrum obtained with a C/5 current was used to identify the series resistance (medium to high frequencies), while the spectrum obtained with a C/50 current was used to identify the surface resistance (low frequencies) (see Fig. 3).

The third part consists of current pulses of 20 seconds followed by a 30 minutes pause around SOC 80%. By analyzing the variation of the voltage during the current pulses, we can extract information about the impedance of the cell. The following currents were tested: -C/2, -1C, -3C, -5C, -8C, +C/2

and +1C, the pulses in charge being applied only at 25°C to avoid lithium-plating, specially in the case of the aged cells presenting a very high impedance. For the other temperatures, the charge current was limited to C/10. This protocol is presented in Fig. 2. The charges between the pulses at -3C, -5C and -8C were omitted to make the figure clearer, but they were done at C/2 (25°C) or C/10 (0°C and 10°C) and recharged the same amount of Ah that had been discharged during the previous pulse. This part of the protocol took 14.5 hours per cell for a total of 17 experimental points, i.e. approximately 51 minutes per point, while the protocol proposed by Damay *et al.* [1] took 150 hours for 70 conditions tested, i.e. 2 hours and 8 minutes per point. The protocol proposed in the present work therefore represents a considerable time saving. The rest time could even be reduced to 15 minutes instead of 30 for current rates inferior to 3C, since temperature and voltage were already stable within this period. This would represent an additional gain of 4.5 hours.

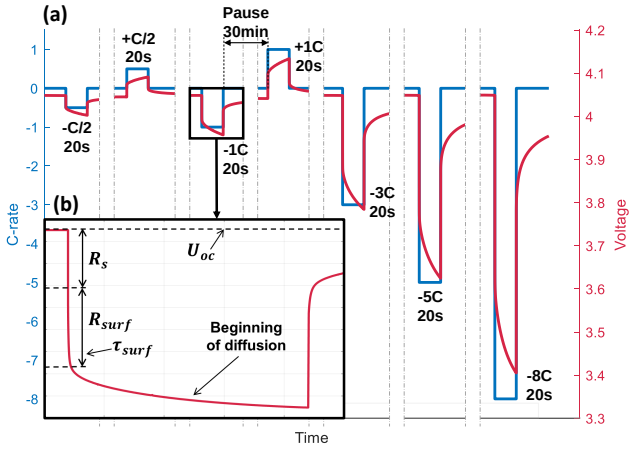

Figure 2: (a) Current pulses protocol and (b) identification of the parameters of the electrical model from the voltage response to a current pulse

2.3 Parameters identification

When characterizing the electrical model, the OCV and the series resistance may be determined first, then the other four parameters are identified simultaneously by fitting.

It is assumed that the series resistance does not depend on the current, so it can be determined from the EIS tests. The surface resistance for a near-zero current can also be identified from EIS. The remaining parameters, including the surface resistance for currents different from near-zero, require current pulses tests to be identified.

2.3.1 Identification from EIS tests

The impedance obtained from an EIS tests is presented in a Nyquist plot, with the real part of its value on the x-axis and the negative of its imaginary part on the y-axis.

R_s and R_{surf} can be determined as represented in Fig. 3.

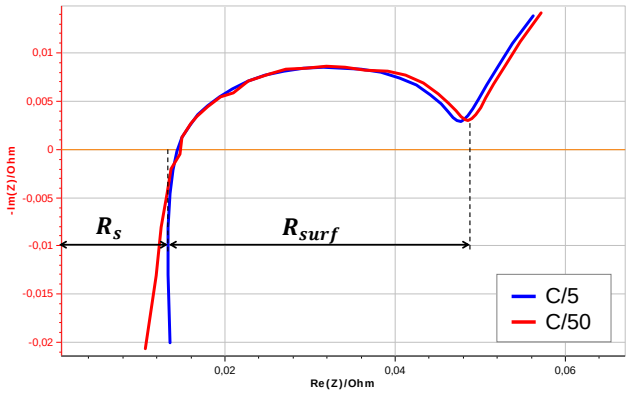

Figure 3: Identification R_s and R_{surf} from an impedance spectrum

2.3.2 Identification from current pulses tests

For this study, the OCV during each pulse is identified by measuring the voltage at the beginning and at the end (after 30 minutes of rest) of the pulse and interpolating these two values. Next, the overvoltage ΔU is calculated by subtracting the OCV from the cell voltage and then fitted to find the remaining parameters using the function fmincon on Matlab using a loss function such as the root mean square error (RMSE). It is modeled by the following equation:

$$\begin{aligned}\Delta\hat{U}(t) = \Bigg[R_s + R_{surf}\left(1 - \exp\left(-\frac{t}{\tau_{surf}}\right)\right) \\ + \sum_{i=1}^{n} R_{diff,i}\left(1 - \exp\left(-\frac{t}{\tau_{diff,i}}\right)\right)\Bigg] I(t)\end{aligned} \tag{1}$$

where n is the number of diffusion circuits (20 for this study). The surface resistance can be determined from the EIS tests as explained in section 2.3.1. Fig. 2 shows the voltage response to a current pulse and gives some indication of which part corresponds to each parameter.

3 Separating SEI and charge transfer contributions to surface resistance

Current dependence for R_{surf} is based on the Butler-Volmer law:

$$I = I_0\left[\exp\left(\frac{(1-\beta)F}{RT}U_{ct}\right) - \exp\left(\frac{-\beta F}{RT}U_{ct}\right)\right] \tag{2}$$

where I_0 is the exchange current $[A]$, β is the transfer coefficient, R is the universal gas constant $[J/(mol \cdot K)]$, T is the temperature $[K]$, F is the Faraday constant $[s \cdot A/mol]$ and U_{ct} $[V]$ is the charge transfer overpotential.

Assuming that the charge transfer coefficient β is equal to 0.5 and knowing that $U_{ct} = U_{surf} - I \cdot R_{SEI}$, the surface resistance can be isolated to find its dependence law on current:

$$R_{surf}(I) = \frac{U_{surf}}{I} = R_{SEI} + \frac{2\,R\,T}{F\,I} \cdot \text{asinh}\left(\frac{I}{2\,I_0}\right) \tag{3}$$

It was demonstrated that R_{SEI} and I_0 are dependent on the temperature in accordance to the Arrhenius Law [1]. In this work, the Arrhenius Law was normalized to display the parameters values at 25°C. This brings the final R_{surf} equation below:

$$\begin{aligned} R_{surf}(I,T) = R_{SEI}(25^{\circ}C) \times \exp\left(\frac{E_{a,SEI}}{k_B}\left(\frac{1}{T} - \frac{1}{298}\right)\right) \\ + \frac{2\,R\,T}{F\,I}\ \text{asinh}\left(\frac{I}{2\,I_0(25^{\circ}C)}\exp\left(\frac{E_{a,I_0}}{k_B}\left(\frac{1}{T} - \frac{1}{298}\right)\right)\right) \end{aligned} \tag{4}$$

where R_{SEI} is the resistance of the SEI layer at 25°C [Ω], $E_{a,SEI}$ and E_{a,I_0} are the activation energies of the considered reactions $[eV]$ and k_B is the Boltzmann constant $[eV/K]$. The first term expresses the contribution of the SEI while the second expresses the contribution of the charge transfer. The parameters to be found are $R_{SEI}(25^{\circ}C)$, $E_{a,SEI}$, $I_0(25^{\circ}C)$ and E_{a,I_0}.

The surface resistance at 25°C (298 K) and zero current is given by:

$$R_{ct,0}(25^{\circ}C) = \frac{R \cdot 298}{F\,I_0(25^{\circ}C)} \tag{5}$$

4 Results and discussion

4.1 Fitting the model to the experimental data

After determining the value of R_{surf} for every test condition, the model described in (4) was fitted to these values using the RMSRE (Root Mean Squared Relative Error) as the loss function. Since the activation energies depend on the chemical reactions occurring in the cell and these reactions are the same regardless its state of health, we decided to impose the same activation energies $E_{a,SEI}$ and E_{a,I_0} for all the SOHs, leaving us with only two parameters to be found in each case, $R_{SEI}(25^{\circ}C)$ and $I_0(25^{\circ}C)$.

Fig. 4 shows the fitting results and the values of the parameters from (4) are presented in Tab. 1. Fig. 5 shows the contributions of SEI layer and charge transfer to the overall surface resistance. Our model performs well for most of the operating conditions tested, except for near-zero current at very low temperature, which will rarely be the operating condition of our application. To improve accuracy in this condition, the RMSE (Root Mean Squared Error) could be used as the loss function. It reduces the absolute error at low temperature and current, to the detriment of the relative error at ambient temperature.

The activation energy $E_{a,SEI}$ is a little lower than the values presented in literature (0.59 eV found by Damay *et al.* [1] and 0.52 eV found by Pinson *et al.* [6]), which can be explained by the differences in the composition of the SEI layer for cells of different chemistries. The value of E_{a,I_0} is close to that proposed by Damay *et al.* [1], 0.81 eV.

4.2 Evolution of surface resistance with aging

The results presented in Tab. 1 show that both SEI and charge transfer resistance increased during cycling aging and calendar aging. In both cases, the increase factor of $R_{ct_0}(25°C)$ is higher than that of

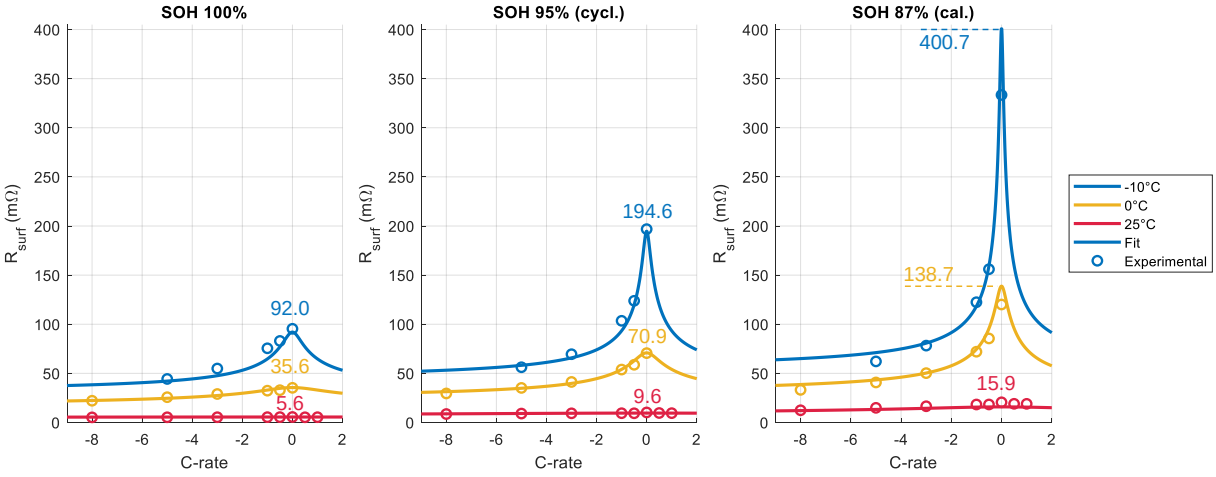

Figure 4: Fitting results for the surface resistance and experimental points for different states of health

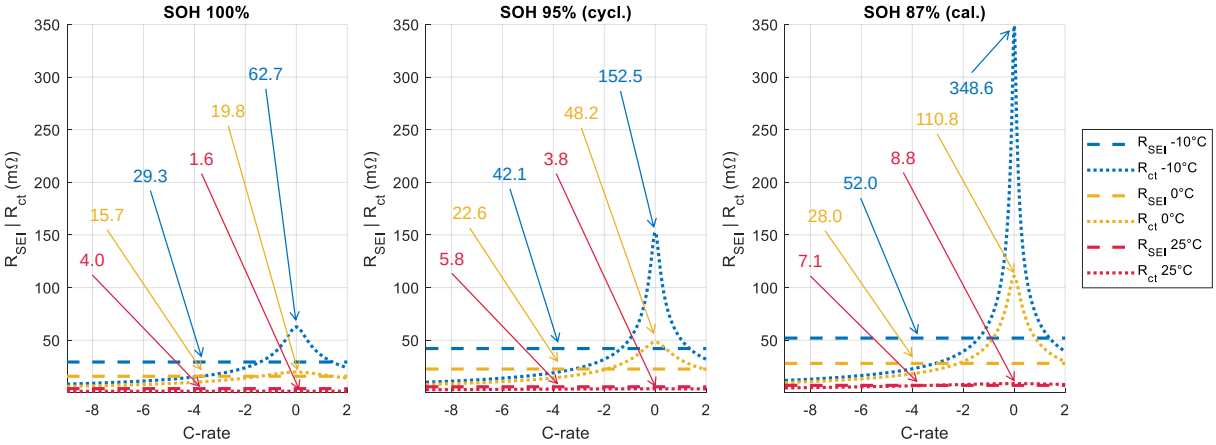

Figure 5: Separation of SEI layer and charge transfer contributions to the surface resistance for different states of health

$R_{SEI}(25°C)$. For SOH 87%, for example, $R_{SEI}(25°C)$ is multiplied by 1.8 while $R_{ct_0}(25°C)$ is multiplied by 5.6. Both aging conditions appear to trigger mechanisms that contribute in a comparable way to the thickening of the SEI layer and the slowdown of charge transfer.

In literature, Wong *et al.* ([7], [8]) found that during cycling aging, the application of high current rates contribute to the rapid formation of a high impedance film, which causes a drastic change in charge transfer kinetics. A significant loss of capacity was observed, as well as a large increase in the charge transfer resistance and a mild growth of the SEI layer. Sabet *et al.* [9] studied NMC cells during cycling aging and observed an increase in charge transfer resistance. The main mechanisms identified were anode's and cathode's particle cracking, cathode dissolution and possibly CEI (Cathode-Electrolyte Interphase) layer growth.

Concerning calendar aging, Stiaszny *et al.* [10] evaluated the impact of storing NCA cells at 60°C at different SOC levels. They observed that the resistances of the SEI layer and the cathode charge transfer

Table 1: Model parameters

Parameter		SOH 100%	SOH 95%	SOH 87%
$\mathbf{R_{SEI}(25°C)}$	$[m\Omega]$	4.00	5.76	7.11
$\mathbf{E_{a,SEI}}$	$[eV]$		0.38	
$\mathbf{I_0(25°}C)$	$[A]$	16.39	6.73	2.93
$\mathbf{E_{a,I_0}}$	$[eV]$		0.74	
$\mathbf{R_{ct_0}(25°C)}$	$[m\Omega]$	1.57	3.82	8.77
RMSRE	[%]	5.93	3.99	12.93
RMSE	$[m\Omega]$	3.48	2.93	17.00

resistance increased. The growth of the SEI layer was even more drastic at higher SOC. Sabet *et al.* [9] observed that both SEI and charge transfer resistances increased for calendar aging.

Our results are therefore coherent, since the calendar aged cell had its SEI and charge transfer resistances increased and the cycled cell presented as well a significant increase in charge transfer. The increase in SEI resistance for the cycled cell might be justified by the long periods at 50°C during the characterization tests, as mentioned in section 2.2.

5 Conclusions

The presented method, originally proposed and applied to an LFP / graphite cell, was successfully transposed to an NCA+NMC / graphite+SiO cell.

Besides, this method makes it possible to separate the contributions of SEI and charge transfer to the global surface resistance as a function of temperature and current, while EIS tests can only inform about what happens at zero current. At ambient temperature, the two resistances are balanced. At low temperatures, R_{ct} increases significantly as current tends towards zero, becoming much higher than R_{SEI}, and this effect is accentuated with aging. As the current increases, R_{ct} tends to a constant value lower than R_{SEI}, which does not depend on the current. These relations may vary for different chemistries.

The evolution of R_{SEI} and R_{ct} during battery aging was characterized and we showed that it is coherent with literature. We found that charge transfer resistance had increased with both cycling and calendar aging. SEI resistance increased in both aging conditions as well, mainly due to the high temperatures to which the cells were subjected in both cases.

Most importantly, it was proved that the proposed model remains consistent at different states of health and that it is easier to recalibrate it comparing to an interpolation table, since the activation energies remain constant as the battery ages, leaving only two parameters to be determined ($R_{SEI}(25°C)$ and $I_0(25°C)$).

6 Perspectives

The relation between the parameters of the proposed model and the SOH could be further developed in order to obtain a state of health estimator. Besides, if R_{surf} can be expressed as a explicit function of SOH, it might be possible to obtain its value for untested SOHs, similarly to what was presented regarding temperature and current.

It may also be possible to embed this method into a BMS in order to do an online recalibration of the surface resistance as the battery ages. It could be done by using current pulses at different temperatures during operation. In this case, the EIS test could be replaced by a very low current pulse. However, this possibility should be investigated based on system limitations, such as sampling rate, sensors accuracy, among other factors.

To complement this work, the dependence on state of charge could also be explored. Besides, the other parameters of the equivalent electric circuit could be studied following physical or behavioral laws.

References

[1] N. Damay, K. M. Mbeya, G. Friedrich, and C. Forgez, "Separation of the charge transfers and solid electrolyte interphase contributions to a battery voltage by modeling their non-linearities regarding current and temperature," *Journal of Power Sources*, vol. 516, p. 230617, 12 2021.

[2] X. Han, M. Ouyang, L. Lu, and J. Li, "Simplification of physics-based electrochemical model for lithium ion battery on electric vehicle. part ii: Pseudo-two-dimensional model simplification and state of charge estimation," *Journal of Power Sources*, vol. 278, pp. 814–825, 3 2015.

[3] G. Dong, X. Zhang, C. Zhang, and Z. Chen, "A method for state of energy estimation of lithium-ion batteries based on neural network model," *Energy*, vol. 90, pp. 879–888, 10 2015.

[4] D. Andre, M. Meiler, K. Steiner, H. Walz, T. Soczka-Guth, and D. U. Sauer, "Characterization of high-power lithium-ion batteries by electrochemical impedance spectroscopy. ii: Modelling," *Journal of Power Sources*, vol. 196, pp. 5349–5356, 6 2011.

[5] M. J. Lain, J. Brandon, and E. Kendrick, "Design strategies for high power vs. high energy lithium ion cells," *Batteries*, vol. 5, 12 2019.

[6] M. B. Pinson and M. Z. Bazant, "Theory of sei formation in rechargeable batteries: Capacity fade, accelerated aging and lifetime prediction," *Journal of The Electrochemical Society*, vol. 160, pp. A243–A250, 2013.

[7] D. N. Wong, D. A. Wetz, A. M. Mansour, and J. M. Heinzel, "The influence of high c rate pulsed discharge on lithium-ion battery cell degradation," vol. 2015-October, Institute of Electrical and Electronics Engineers Inc., 10 2015. 17.

[8] D. Wong, B. Shrestha, D. A. Wetz, and J. M. Heinzel, "Impact of high rate discharge on the aging of lithium nickel cobalt aluminum oxide batteries," *Journal of Power Sources*, vol. 280, pp. 363–372, 4 2015. 63.

[9] P. S. Sabet, A. J. Warnecke, F. Meier, H. Witzenhausen, E. Martinez-Laserna, and D. U. Sauer, "Non-invasive yet separate investigation of anode/cathode degradation of lithium-ion batteries (nickel–cobalt–manganese vs. graphite) due to accelerated aging," *Journal of Power Sources*, vol. 449, p. 227369, 2 2020. 59.

[10] B. Stiaszny, J. C. Ziegler, E. E. Krauß, M. Zhang, J. P. Schmidt, and E. Ivers-Tiffée, "Electrochemical characterization and post-mortem analysis of aged limn2o4–nmc/graphite lithium ion batteries part ii: Calendar aging," *Journal of Power Sources*, vol. 258, pp. 61–75, 7 2014. 57.